SUPPLEMENTARY MATERIAL

Spatiotemporal patterns of rain-on-snow and basal ice in high Arctic Svalbard: detection of a climate-cryosphere regime shift

Bart Peeters*, Åshild Ønvik Pedersen, Leif Egil Loe, Ketil Isaksen, Vebjørn Veiberg, Audun Stien, Jack Kohler, Jean-Charles Gallet, Ronny Aanes, Brage Bremset Hansen

Table of Contents

1. Data overview

Data collection

In Central Spitsbergen, sampling was conducted annually at the same sites (*n* = 128), which were spatially structured following a hierarchical block design across eight different locations (figure 2(c), table S1.1). At each location, sample plots covered two different vegetation types (ridge and sub-ridge) approximately 5 m apart, replicated at 50 m and 500 m distance, as well as two elevations covering the valley bottom and flat hilltops (mean = 112 and 203 m above sea level (a.s.l.), respectively), i.e. 2 x 2 x 2 x 2 = 16 plots (see Loe et al., 2016).

On the NW coast, data collection from 2013-2017 followed a similar hierarchical design as in Central Spitsbergen with *n* = 16 and 24 plots at the southern and northern side of Brøggerhalvøya, respectively, covering three elevations: valley bottom, flat hilltop, and mountain summit (mean = 34, 179 and 444 m a.s.l., respectively). From 2005-2012 (except 2009), sampling was conducted at fixed sites in a randomly placed grid system covering vegetated terrain < 200 m a.s.l. in Brøggerhalvøya (*n* = 14-28 plots), Sarsøyra (*n* = 22-33) and Kaffiøyra (*n* = 13-18) (figure 2(b); Hansen et al., 2011). In addition, as part of another study (see Kohler and Aanes, 2004), cryosphere data was collected in Brøggerhalvøya (total *n* = 1,031 over the years 2000, 2002-2007, 2010, 2012-2015) along transect lines with sampling locations varying among years. For simplicity, sampling sites in Brøggerhalvøya were grouped in three main locations: the flat, rocky shore at Kvadehuken in North-West Brøggerhalvøya, and the coastlines of North and South Brøggerhalvøya. Thus, sampling sites were grouped into thirteen locations: eight locations in Central Spitsbergen following the hierarchical sampling design, and five locations on the NW coast, i.e. Sarsøyra, Kaffiøyra and three locations on Brøggerhalvøya (table S1.1).

Table S1.1: Number of sample plots for snow and basal ice measurements (April/early May) per year and location.

Study Area	Area	Location	Latitude	Longitude	2000	2002	2003	2004	2005	2006	2007	2008	2010	2011	2012	2013	2014	2015	2016	2017
NW coast	Brøggerhalvøya	Kvadehuken	78.95 N	11.45 E	19	13	21	16	13*	22*	15*	-	21*	4	59*	94*	13*	98*	-	-
		North Brøgger	78.94 N	11.78 E	21	10	23	11	14*	64*	14*	-	28*	5	61*	96*	32*	118*	22	20
		South Brøgger	78.88 N	11.60 E	16	14	18	23	14*	10	18*	-	34*	5	44*	71*	25*	79*	16	16
	Sarsøyra	Sarsøyra	78.75 N	11.70 E	-	-	-	-	33	22	22	22	22	22	22	-	-	-	-	-
	Kaffiøyra	Kaffiøyra	78.64 N	11.95 E	-	-	-	-	18	18	18	16	15	13	15	-	-	-	-	-
Central	Colesdalen	Colesbay	78.11 N	15.06 E	-	-	-	-	-	-	-	-	16	16	16	16	16	16	16	16
Spitsbergen		Fardalen-Bødalen	78.10 N	15.34 E	-	-	-	-	-	-	-	-	16	-	16	16	16	16	16	16
		Medalen	78.05 N	15.46 E	-	-	-	-	-	-	-	-	16	16	16	16	16	16	16	15
	Semmeldalen	Istjørndalen	78.02 N	15.23 E	-	-	-	-	-	-	-	-	16	-	-	16	16	16	16	16
		Semmelbu	78.00 N	15.36 E	-	-	-	-	-	-	-	-	16	-	15	16	16	16	16	16
		Semmeldalen	77.96 N	15.44 E	-	-	-	-	-	-	-	-	16	-	16	16	16	14	16	8
	Reindalen	Gangdalen	77.99 N	15.78 E	-	-	-	-	-	-	-	-	16	-	16	16	16	16	16	16
		North Reindalen	77.96 N	15.64 E	-	-	-	-	-	-	-	-	16	16	16	16	16	16	16	16

* Sample size is a combination of snow pits randomly placed along transect lines, and annually repeated snow pits at fixed points from either a randomly placed grid (2005-2007, 2010, and 2012) or the hierarchical block design (2013-2015).

Table S1.2: Information on meteorological stations with the period (years) for which data on both daily average temperature and total precipitation were available. Altitude is given in meters above sea level.

Meteorological station	Period	Altitude	Latitude	Longitude	Source	URL
Ny-Ålesund [a]	1969-2017	8 m	78.92 N	11.93 E	Norwegian Meteorological Institute	eklima.met.no
Svalbard Airport [a, b]	1957-2017	28 m	78.25 N	15.50 E	Norwegian Meteorological Institute	eklima.met.no
Hopen	1945-2017	6 m	76.51 N	25.01 E	Norwegian Meteorological Institute	eklima.met.no
Isfjord Radio	1946-1976; 2015-2017	7 m	78.06 N	13.62 E	Norwegian Meteorological Institute	eklima.met.no
Sveagruva	1978-2001	9 m	77.90 N	16.72 E	Norwegian Meteorological Institute	eklima.met.no
Barentsburg	1973-1992; 2003-2017	40 m	78.06 N	14.21 E	Tutiempo Network, S.L.	https://en.tutiempo.net/climate/ws-201070.html
Hornsund	1979-2016	10 m	77.00 N	15.54 E	Institute of Geophysics, Polish Academy of Sciences	–

a - Meteorological stations used for the basal ice analyses at the NW coast (Ny-Ålesund) and Central Spitsbergen (Svalbard Airport) study areas;
b - the Svalbard Airport composite series (1957-2017) comprises data from the nearby meteorological station in Longyearbyen (1957-1975) and at Svalbard Airport (1975-2017), and is considered to be homogenous (collectively referred to as Svalbard Airport) (Nordli et al., 2014).

2. Details on the data analysis

Regression analyses

We compared annual basal ice occurrence (presence/absence, where presence ≥ 0.5 cm basal ice) between the study areas for the period 2010-2017 by using a generalized linear model (GLM; binomial distribution and logit link function) with the categorical variables Study Area and Year, and their interaction, as predictor variables. Similarly, we compared annual basal ice thickness (cm, log-transformed after adding one to avoid log of zero) between the study areas using an ANOVA with the same predictors.

We used a multiple linear regression model (LM) to analyze how average snow depth measured in late winter (April/early May) for the NW coast (n = 16 years) and Central Spitsbergen (n = 8 years) is correlated with average basal ice thickness. Here, we included average observed basal ice thickness and Study Area as predictor variables, also accounting for cumulative snowfall (November-March).

To analyze the effects of climate and topography on the occurrence of basal ice, we used generalized linear mixed models (GLMM) with binomial distribution (presence/absence) and logit link function. For the analysis of basal ice thickness, we used linear mixed models (LMM) with Gaussian distribution. Mixed-effects models were implemented using the *lme4* package (Bates et al., 2015) in R version 3.3.2 (R Core Team, 2016). Since the ice data covered only 16 years, we avoided over-parameterization by restricting the number of climate parameters (including intercept) to be estimated by the model to four. The fixed climate effects considered in the model were either Rain, Snow_P and their interaction, or Rain, Heat sum and their interaction. Elevation (m a.s.l.) and Slope (degrees) at the plot-level, derived from a Digital Elevation Model with a 20 m resolution (http://geodata.npolar.no), were also included as fixed effects to estimate topographic effects on basal ice. Since precipitation is more likely to fall as snow at higher altitude (van Pelt et al., 2016), we also considered a two-way interaction between Rain and Elevation. In both models, we included the following variables as random effects on the intercept: Year (*n* = 16), to account for dependency of observations taken within the same year; Location (*n* = 13; table S1.1), to account for spatial autocorrelation and different sampling design among areas; and Plot ID (*n* = 1,282), to account for dependency among the observations in the fixed plots. Basal ice thickness, Rain and Snow_P were log-transformed (after adding one to avoid log of zero) in the analyses. Covariates were standardized in the models for comparison. We performed model selection based on Akaike's Information Criterion (AIC; Burnham and Anderson, 2002; supplementary material 4). For the LMM of basal ice thickness, model selection was performed on models fitted using maximum likelihood, while the parameter estimates for the selected models were obtained after refitting the models using restricted maximum likelihood (REML; Verbeke and Molenberghs, 2000). We also calculated estimates of R^2 following Nakagawa and Schielzeth (2013) and performed cross-validation of the models by excluding one year at a time (i.e., leave-one-out cross-validation) to evaluate robustness of parameter estimates and model predictions (supplementary material 5).

Spatial correlation

To analyze patterns of spatial correlation of annual fluctuations in winter rain and basal ice, we used a nonparametric covariance function that uses smoothing splines to analyze spatial covariance as a function of distance (Bjørnstad and Falck, 2001) implemented in the R-package *ncf* (Bjørnstad, 2016). This method estimates local and regional correlation based on pairwise correlations and distances among sample plots (or meteorological stations for winter rain). We set a criterion of at least five years of overlapping data within the available time-series to calculate pairwise correlations. This left us with 19 pairwise correlations of winter rain time-series from seven different meteorological stations covering distances of 14 - 410 km. For basal ice, spatial correlation was first analyzed separately for the two study areas. For Central Spitsbergen, we obtained 8,035 pairwise correlations from 128 plots with distances ranging up to 22 km. For the NW coast, only data of fixed plots (i.e. following the hierarchical or random grid design) was used, leaving us with 1,676 pairwise correlations from 82 plots with distances up to 45 km (covering the period 2005-2017, except 2009). Thereafter, we combined data from both study areas (for the period 2010-2017) to analyze spatial correlation in basal ice up to 142 km in distance between sampling plots. To investigate the contribution of rain to spatial correlation in basal ice, we fitted log-linear models of basal ice thickness with Rain as a predictor for every plot (2010-2017), using weather data from Svalbard Airport and Ny-Ålesund for Central Spitsbergen and NW coast, respectively. We then analyzed spatial correlation in annual fluctuations of the residuals from these models. The maximum degrees of freedom for the smoothing spline was set to three and confidence intervals around the nonparametric curve were calculated by bootstrapping the analysis using 100 and 1,000 iterations for spatial correlation in basal ice and winter rain, respectively (Bjørnstad and Falck, 2001).

Regime shifts

Basal ice occurrence and thickness were estimated using historical weather data (since 1957 and 1969 for Svalbard Airport and Ny-Ålesund, respectively) after refitting the selected mixed-effects models using unstandardized covariates. For years when no rain events occurred, Snow_P was equivalent to the total amount of snowfall (November-March). We then tested for regime shifts (i.e. inter-decadal fluctuations in average climatic levels; Overland et al., 2006) in winter rain and modelled basal ice using the Binary Segmentation method in the *cpt.mean* function implemented in the R-package *changepoint* (Killick et al., 2016). Minimum segment length was set to five years and the maximum number of change points was restricted based on the breakpoint in the curve of the change points' penalty values.

3. Snow depth – basal ice: regression parameters

Table S3: Parameter estimates (β) with standard errors (SE) from the linear regression model of average snow depth (cm; measured in April/early May) in relation to basal ice thickness (cm), study area (as a categorical variable) and cumulative snowfall (mm: November-March), which was standardized within each study area. The intercept is given for the NW coast study area.

Parameter	β	SE	*P*-value
Intercept (NW coast)	58.50	6.83	< 0.001
Study area (Central Spitsbergen)	-20.30	7.36	0.012
Basal ice thickness	-2.41	0.87	0.012
Snowfall	3.70	3.07	0.242

4. Model selection

Model selection for the analysis of basal ice thickness resulted in only one top-ranked model (*ΔAIC* > 2 for all other models; table S4.1), whereas five candidate models were selected for the analysis of basal ice occurrence (table S4.2(a)). These models included either the climatic variables Rain in interaction with Snow_P, or Rain with an additive effect of Heat sum. However, when excluding data from 2017 from the analysis, models including an additive effect of Snow_P outperformed models including Heat sum (table S4.2(b)). Therefore, and because the interaction between Rain and Snow_P was also included in the selected model for basal ice thickness, historical basal ice occurrence was modelled using the estimates from the top ranked model based on the full data set (table S4.2(a); table 1 in the main text).

Table S4.1: Model selection based on Akaike's Information criterion (AIC) for the fixed effects on basal ice thickness (LMM), showing the top ten candidate models. All models included Year, Location and Plot ID as random effects on the intercept.

Model rank	Elevation	Slope	Rain	Snow_P	Heat sum	Rain : Elevation	Rain : Snow_P	Rain : Heat sum	*AIC*	*ΔAIC*	Log Likeli-hood
1	x	x	x	x		x	x		5583.00	0.00	-2780.50
2	x	x	x		x	x		x	5588.95	5.95	-2783.48
3	x	x	x		x	x			5598.05	15.05	-2789.03
4	x	x	x			x			5604.22	21.22	-2793.11
5	x	x	x	x		x			5605.95	22.95	-2792.98
6	x		x	x		x	x		5615.66	32.66	-2797.83
7	x	x	x	x			x		5621.86	38.86	-2800.93
8	x		x		x	x		x	5623.73	40.73	-2801.86
9	x		x		x	x			5632.88	49.88	-2807.44
10	x		x			x			5639.71	56.71	-2811.86

Table S4.2: Model selection based on Akaike's Information criterion (AIC) for the fixed effects on basal ice occurrence (binomial GLMM), showing the top ten candidate models for (a) the full data set, and (b) time-series excluding winter 2016/2017. All models included Year, Location and Plot ID as random effects on the intercept.

Model rank	Elevation	Slope	Rain	Snow_P	Heat sum	Rain : Elevation	Rain : Snow_P	Rain : Heat sum	*AIC*	*ΔAIC*	Log Likeli-hood
(a) full data set											
1	x	x	x	x			x		1953.10	0.00	-967.55
2	x	x	x	x		x	x		1953.70	0.60	-966.85
3	x	x	x		x	x			1954.69	1.59	-968.34
4	x	x	x		x				1954.96	1.86	-969.48
5	x		x	x			x		1954.96	1.86	-969.48
6	x		x	x		x	x		1955.67	2.57	-968.84
7	x		x		x	x			1956.09	2.99	-970.04
8	x		x		x				1956.26	3.16	-971.13
9	x	x	x		x	x		x	1956.65	3.55	-968.33
10	x	x	x	x		x			1956.80	3.70	-969.40
(b) excluding winter 2016/2017											
1	x	x	x	x		x			1736.62	0.00	-859.31
2	x		x	x		x			1738.03	1.41	-861.01
3	x	x	x	x		x	x		1738.62	2.00	-859.31
4	x		x	x		x	x		1740.01	3.39	-861.01
5	x	x	x	x					1740.63	4.01	-862.31
6	x		x	x					1741.91	5.29	-863.96
7	x	x	x	x			x		1742.19	5.57	-862.10
8	x		x	x			x		1743.35	6.73	-863.67
9	x	x	x			x			1744.76	8.14	-864.38
10	x		x			x			1746.15	9.53	-866.08

5. Cross-validation

We checked whether the parameter estimates for basal ice occurrence and thickness were sensitive to observed weather variables in certain years. This could indicate how, for example, a year with a very early rain event and hence low accumulated snowfall (Snow_P) can influence the overall interpretation of the results. Therefore, we performed cross-validation by excluding one year at a time from the analysis (i.e., leave-one-out cross-validation) to detect systematic deviations in parameter estimates. Confidence intervals of fixed effect estimates were approximated using Wald's method implemented in the *confint* function in the R-package *lme4* (Bates et al., 2015), which is computationally much faster than parametric bootstrapping. We also predicted basal ice occurrence/thickness for the year that was left out, and compared it with the observed mean and predicted response based on the full model.

Overall, cross-validation revealed few systematic deviations in parameter estimates and predictions among years (figures S5.1-4). Average observed basal ice thickness was strongly correlated (Pearson's r = 0.91) with predictions based on the full data set, and with cross-validated predictions (i.e. when basal ice was predicted for each year based on a model where this year was excluded; r = 0.84). Similarly, the correlation between average observed and predicted basal ice occurrence was 0.93 when modelling the full data set and 0.87 when based on cross-validated predictions. This indicates that our models were highly robust.

When excluding 2012 from the model for basal ice thickness, the interaction between rain and Snow_P and additive effect of Snow_P became considerably stronger (figure S5.1). This year was characterized by a record mid-winter warm spell and extreme rain event leading to the strongest observed basal ice occurrence and thickness in both study sites (figure 3 in main text; Hansen et al., 2014). However, the difference in predicted basal ice thickness with and without 2012 was small (figure S5.2). For the analysis of basal ice occurrence, cross-validation indicated that the interaction between rain and Snow_P was no longer significant when excluding data from 2017 (figures S5.3-4). This year was characterized by very low Snow_P due to an early major rain event, and a very high cumulative heat sum (the mildest winter recorded at Svalbard Airport in that study period; figure 3 in main text). However, the prediction of basal ice occurrence was strongly overestimated for Svalbard Airport 2017 when this year was not included in the model (figure S5.4(b)). In addition, when excluding this year, the interaction effect between rain and Snow_P on basal ice occurrence became less important in the model selection (table S5.1). Therefore, while the interaction of rain with snow cover seems an overall important determinant for basal ice thickness, snow and rain have primarily additive effects on basal ice occurrence.

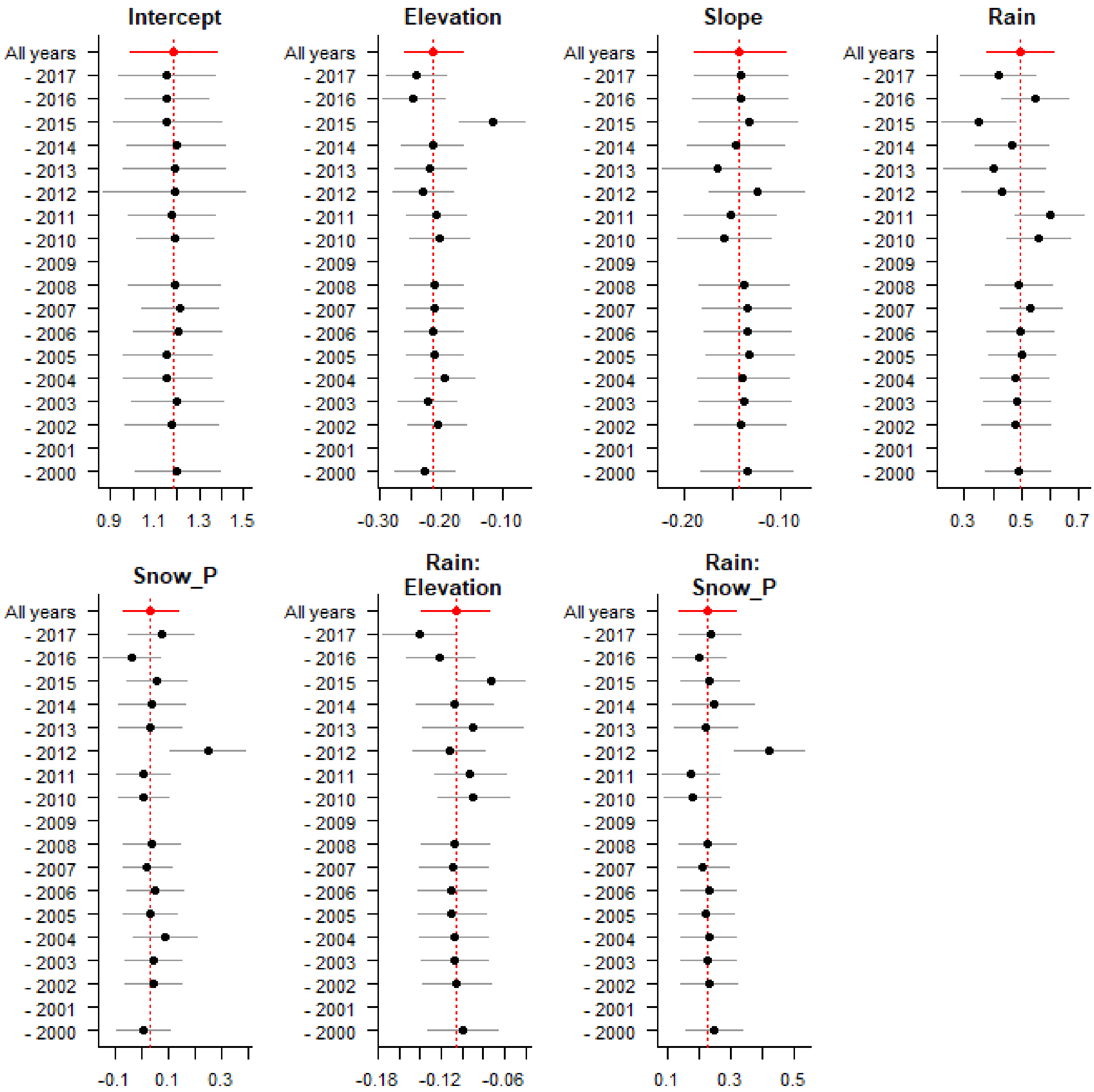

Figure S5.1: Cross-validation of basal ice thickness showing parameter estimates of fixed effect covariates when excluding one year at a time (indicated on the y-axis). Horizontal lines show 95% CIs. Estimates are shown for standardized variables. Red symbols indicate estimates of the model including all years.

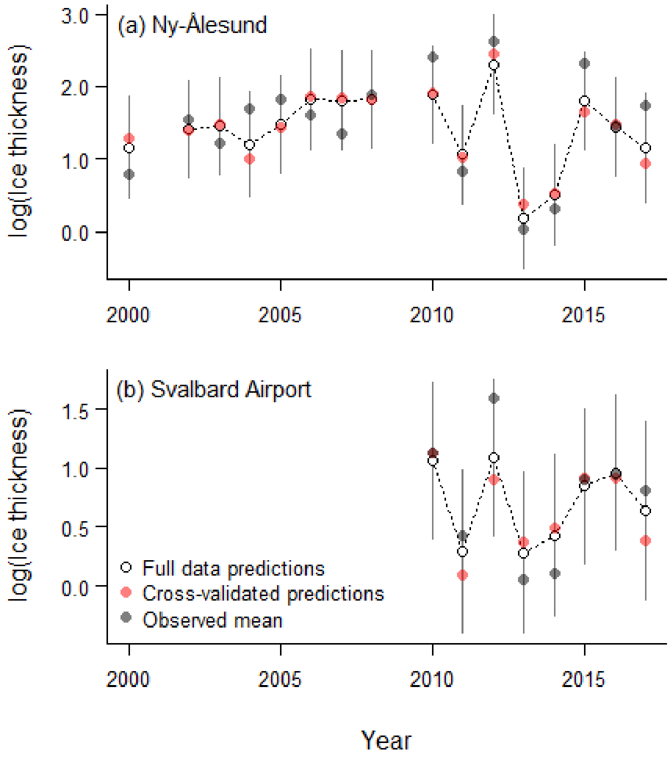

Figure S5.2: Observed and predicted (i.e. modelled) basal ice thickness (natural logarithmic scale) for meteorological stations in (a) Ny-Ålesund, NW coast, and at (b) Svalbard Airport, Central Spitsbergen. Red dots indicate predicted mean basal ice thickness for a given year based on a model where this year was excluded. Open dots and vertical lines indicate predicted values with 95% prediction intervals based on the top ranked model including all years. Grey dots indicate mean observed basal ice thickness.

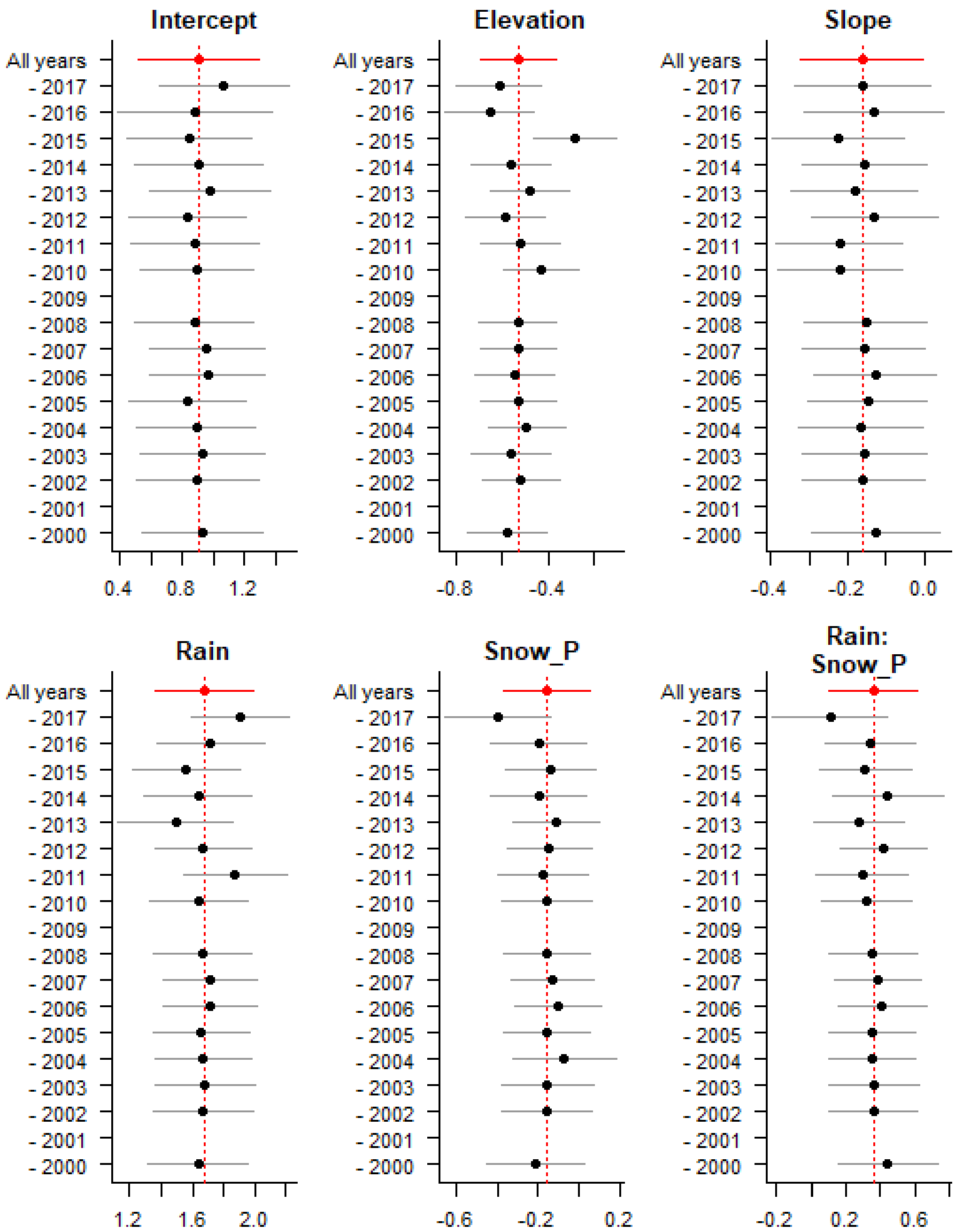

Figure S5.3: Cross-validation of basal ice occurrence showing parameter estimates of fixed effect covariates when excluding one year at a time (indicated on the y-axis). Horizontal lines show 95% CIs. Estimates are shown for standardized variables. Red symbols indicate estimates of the model including all years.

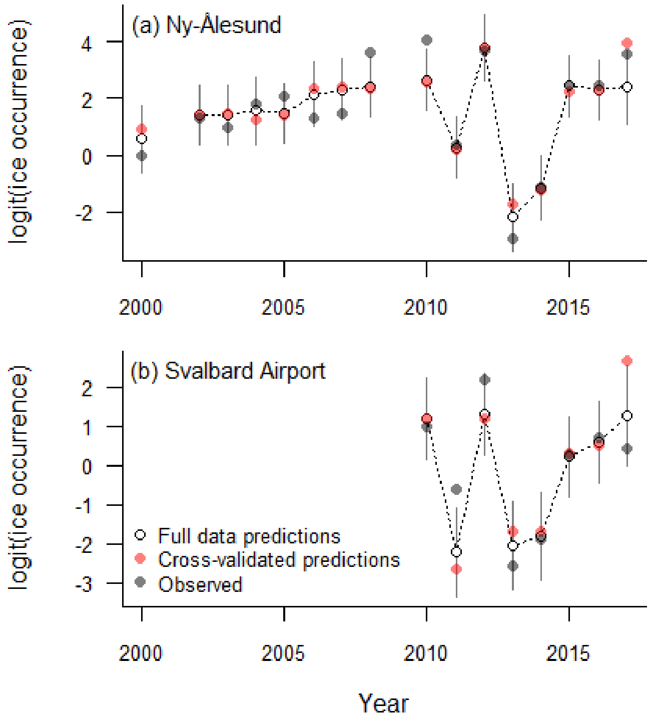

Figure S5.4: Observed and predicted (i.e. modelled) basal ice occurrence (on logit scale) for the meteorological stations in (a) Ny-Ålesund, NW coast, and at (b) Svalbard Airport, Central Spitsbergen. Red dots indicate predicted mean basal ice occurrence for a given year based on a model where this year was excluded. Open dots and vertical lines indicate predicted values with 95% prediction intervals based on the top ranked model including all years. Grey dots indicate mean observed basal ice occurrence.

6. Spatial correlation: total study area

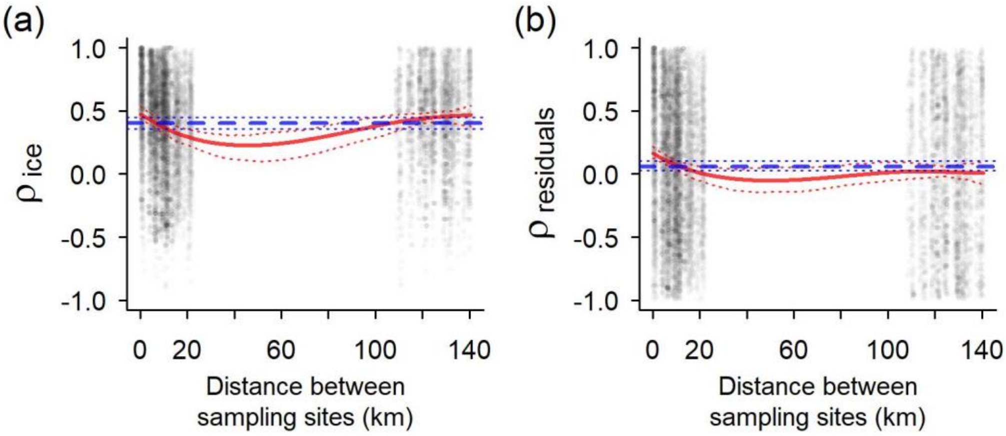

Figure S6: Spatial correlation across the total study area in annual fluctuations of (a) basal ice thickness and (b) residuals in basal ice thickness after accounting for the effect of winter rain. Dots indicate pairwise correlations between sampling sites. The dashed blue line shows the average spatial, i.e. “regional”, correlation, while the solid red line shows the nonparametric covariance as a function of distance, both with 95% CI (dotted lines).

7. Within-snowpack ice thickness

Methods

During fieldwork in April/early May, the total thickness of ice layers within the snowpack was measured in Central Spitsbergen (n = 128; 2010-2017) and on the NW coast (n = 251 unique sites; 2005-2017, except 2009). Here, we provide an explorative analysis to support our interpretation of how within-snowpack ice formation varies with snow depth and the amount of winter rain. We ran a linear mixed model (LMM) for total within-snowpack ice thickness (cm; log-transformed after adding one unit to avoid log of zero). Similar to the analysis of basal ice occurrence and thickness, we included Year, Location and Plot ID as random effects on the intercept. Elevation and Slope were included to correct for topographic effects, and Rain and Snow_P (i.e., cumulative snowfall from 1 November until the peak rain event) as climatic variables. We also included two-way interactions between Rain and Snow_P, and Rain and Elevation. Also, a quadratic effect of Rain was included since rain is expected to percolate through the entire snowpack when substantial quantities of rain fall (Putkonen and Roe, 2003), thus creating more ice at the snow/ground interface than within the snowpack. Since the ice layer data only includes twelve years of data, the model is over-parametrized (four annual climatic variables) and estimates must therefore be interpreted with caution. However, this supplementary analysis is included for explorative reasons and we, therefore, chose to report estimates of the global model rather than performing full model selection.

Results and discussion

Firstly, total within-snowpack ice thickness, observed in April/early May, increased strongly with cumulative snowfall until the peak rain event (Snow_P), as within snowpack ice formation is inherently dependent on the snowpack thickness (table S7). However, this effect of Snow_P decreased with increasing amount of rain, and there was a strong negative quadratic effect of

Rain on within-snowpack ice thickness (table S7, figure S7). These observed patterns likely reflect the process of rain percolating through the entire snowpack during extreme rain events (Putkonen and Roe, 2003, Würzer et al., 2016), which is coherent with the observed positive effect of Rain and the positive interaction between Rain and Snow_P on basal ice thickness and occurrence (see table 1 and figure 5 in main paper). The positive interaction effect between Elevation and Rain (table S7) may again indicate that, during a warm spell with air temperatures above freezing at lower elevations, precipitation is more likely to fall as snow or wet snow at higher elevations.

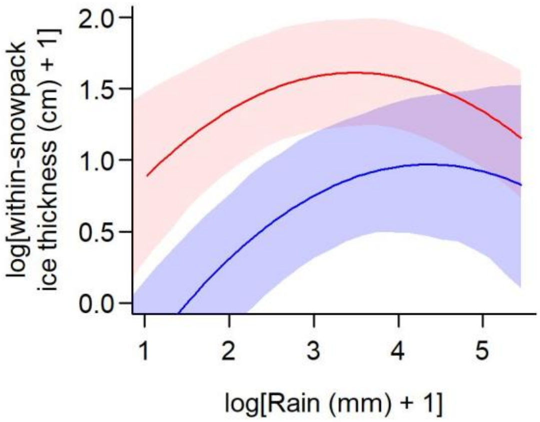

Figure S7: Total within-snowpack ice thickness (cm, on log scale) as a function of winter rain (mm, log scale). Red and blue lines are for, respectively, high and low (mean ± 1SD) accumulated snowfall until the peak rain event (Snow_P), with 95% CI indicated by shaded areas.

Table S7: Parameter estimates (β) and standard errors (SE) of standardized covariates from the mixed-effects model on total within-snowpack ice thickness. Rain, Snow_P (i.e. accumulated snowfall until the peak rain event) and within-snowpack ice thickness were log-transformed after adding one unit to avoid log of zero. Standard deviations (SD) and number of groups (*n*) are given for the random effects on the intercept. Marginal and conditional R^2 indicate variance explained by the fixed effects and by both fixed and random effects, respectively (Nakagawa and Schielzeth, 2013).

Fixed effects	$\beta \pm SE$	*P*-value	**Random effects**	SD	*n*
Intercept	1.308 ± 0.171	<0.001	Year	0.558	12
Elevation	-0.030 ± 0.036	0.400	Location	0.108	13
Slope	-0.071 ± 0.035	0.044	Plot ID	0.310	251
Rain	0.129 ± 0.082	0.117			
Snow_P	0.326 ± 0.074	<0.001			
$Rain^2$	-0.224 ± 0.044	<0.001			
Rain : Snow_P	-0.126 ± 0.078	0.109		Marginal	Conditional
Rain : Elevation	0.083 ± 0.020	<0.001	$\boldsymbol{R^2}$	0.204	0.638

References

Bates, D., Maechler, M., Bolker, B. & Walker, S. 2015. Fitting linear mixed-effects models using lme4. *Journal of Statistical Software,* 67**,** 1-48.

Bjørnstad, O. N. 2016. ncf: Spatial Nonparametric Covariance Functions. R package version 1.1-7.

Bjørnstad, O. N. & Falck, W. 2001. Nonparametric spatial covariance functions: Estimation and testing. *Environmental and Ecological Statistics,* 8**,** 53-70.

Burnham, K. P. & Anderson, D. R. 2002. *Model selection and multimodel inference: a practical information-theoretic approach,* New York, Springer, New York.

Hansen, B. B., Aanes, R., Herfindal, I., Kohler, J. & Sæther, B.-E. 2011. Climate, icing, and wild arctic reindeer: past relationships and future prospects. *Ecology,* 92**,** 1917-1923.

Hansen, B. B., Isaksen, K., Benestad, R. E., Kohler, J., Pedersen, Å. Ø., Loe, L. E., Coulson, S. J., Larsen, J. O. & Varpe, Ø. 2014. Warmer and wetter winters: characteristics and implications of an extreme weather event in the High Arctic. *Environmental Research Letters,* 9**,** 114021.

Killick, R., Haynes, K. & Eckley, I. 2016. Changepoint: An R package for changepoint analysis. R package version 2.2.2.

Kohler, J. & Aanes, R. 2004. Effect of winter snow and ground-icing on a Svalbard reindeer population: Results of a simple snowpack model. *Arctic, Antarctic, and Alpine Research,* 36**,** 333-341.

Loe, L. E., Hansen, B. B., Stien, A., D. Albon, S., Bischof, R., Carlsson, A., Irvine, R. J., Meland, M., Rivrud, I. M., Ropstad, E., Veiberg, V. & Mysterud, A. 2016. Behavioral buffering of extreme weather events in a high-Arctic herbivore. *Ecosphere,* 7**,** e01374.

Nakagawa, S. & Schielzeth, H. 2013. A general and simple method for obtaining R2 from generalized linear mixed-effects models. *Methods in Ecology and Evolution,* 4, 133-142.

Nordli, O., Przybylak, R., Ogilvie, A. E. J. & Isaksen, K. 2014. Long-term temperature trends and variability on Spitsbergen: the extended Svalbard Airport temperature series, 1898-2012. *Polar Research,* 33, 21349.

Overland, J. E., Percival, D. B. & Mofjeld, H. O. 2006. Regime shifts and red noise in the North Pacific. *Deep Sea Research Part I: Oceanographic Research Papers,* 53, 582-588.

Putkonen, J. & Roe, G. 2003. Rain-on-snow events impact soil temperatures and affect ungulate survival. *Geophysical Research Letters,* 30, 1188–1192.

R Core Team 2016. R: A language and environment for statistical computing. R Foundation for Statistical Computing, Vienna, Austria.

Van Pelt, W. J. J., Kohler, J., Liston, G. E., Hagen, J. O., Luks, B., Reijmer, C. H. & Pohjola, V. A. 2016. Multidecadal climate and seasonal snow conditions in Svalbard. *Journal of Geophysical Research: Earth Surface*, 121, 2100-2117.

Verbeke, G. & Molenberghs, G. 2000. *Linear mixed models for longitudinal data,* New York, Springer-Verlag.

Würzer, S., Jonas, T., Wever, N. & Lehning, M. 2016. Influence of initial snowpack properties on runoff formation during rain-on-snow events. *Journal of Hydrometeorology,* 17, 1801-1815.